ELSEVIER

Surface Science 432 (1999) 279–290

surface science

www.elsevier.nl/locate/susc

Adsorption of the formate species on copper surfaces: a DFT study

J.R.B. Gomes, J.A.N.F. Gomes *

CEQUP/Departamento de Química, Faculdade de Ciências, Universidade do Porto, Rua do Campo Alegre, 687, 4169-007 Porto, Portugal

Received 16 January 1999; accepted for publication 22 April 1999

Abstract

The density functional theory and the cluster model approach have been applied to study the interaction of the formate species with the copper (100), (110) and (111) surfaces. The short-bridge, long-bridge and cross-bridge sites of the copper surface have been modelled by Cu_7 and Cu_8 metal clusters after checking the validity of the results against those obtained with much larger clusters. The results show that the formate species is stabilized strongly on the short-bridge site of the surfaces considered and this is in agreement with available experimental data. For adsorption on the short-bridge site, and for the three surfaces considered, the Cu_{surf}—O is close to 2.02 Å, the C—O bond length is 1.26 Å and the O—C—O angle is 128°. On this adsorption site, formate is bridge-bonded with the two oxygens almost in a top position on two copper atoms. For the long-bridge site, the oxygen atoms of the adsorbate are not located above the two copper atoms. The two O—C bonds are equivalent when formate is adsorbed on these two sites. On the cross-bridge site, the formate species is bonded to the surface in a monodentate conformation. The two O—C bonds are different with two clearly different bond lengths. The difference is larger for adsorption on the Cu (100) surface. In this case, the bond lengths are typical of a bond order of one and two. The bonding to the surface is essentially ionic, and the total charge in the adsorbate is 0.75 $\pm$0.05 *e*, approximately.

Keywords: Chemisorption; Copper; Cu; DFT; HCO_2; Heterogeneous catalysis; Theoretical study; Vibrations of adsorbed molecules

1. Introduction

The decomposition of formic acid on metal surfaces has been the subject of numerous experimental studies in recent years [1–27], due to the simplicity of the intermediates and products involved.

Formate is observed during the methanol oxidation reaction, and it is thought to be an intermediate in the methanol synthesis reaction. The most extensively studied surfaces are those directly related to the catalysis of these two reactions, i.e. copper and silver. In industry, a silver catalyst is used to obtain formaldehyde from methanol and a Cu/ZnO catalyst to produce methanol from syn-gas.

Surface formate is easily formed from formic acid by O—H bond cleavage. It can undergo dehydrogenation to produce H_2 and CO_2 and dehydration to yield H_2O and CO, depending on the metal surface. On copper surfaces, only dehydrogenation is observed [1,8]. Formate has been studied by different experimental techniques on

* Corresponding author. Fax: +351-2-6082959.
E-mail address: jfgomes@fc.up.pt (J.A.N.F. Gomes)

0039-6028/99/$ – see front matter
PII: S0039-6028(99)00605-6

copper (100) [1–7], copper (110) [5–22], copper (111) [23] and supported copper surfaces [23–27]. HCO_2 has been identified by temperature-programmed reaction spectroscopy (TPRS) [8,9], by electron energy loss spectroscopy (EELS) [1], high-resolution electron energy loss spectroscopy (HREELS) [1,8], reflection absorption infra-red spectroscopy (RAIRS) [10], in-situ infra-red reflection absorption spectroscopy (IRAS) [10,11,23] and scanning tunnelling microscopy (STM) [12–14]. From the results obtained with these techniques, it was difficult to clarify how the formate species are chemisorbed on copper surfaces, if formate were bonded to the copper surfaces in a upright or tilted geometry or if it were bonded in a bidentate or monodentate geometry. This is due to the observation, or not, of the υ_{as} (OCO) band. More studies were performed using near-edge X-ray absorption spectroscopy (NEXAFS) [3,4,15,16], and it was concluded that the formate species was oriented with its molecular plane normal to the metal surface. By means of surface extended X-ray absorption fine structure (SEXAFS) [3,4], it was found that the HCO_2 species was adsorbed on the Cu (100) surface on the cross-bridge site and later, in a data reanalysis [5,6], that the diagonal atop site was the preferred adsorption site for formate adsorption. On the Cu (110) surface, the aligned atop site [5,6,15,16] seemed to be the most favourable for HCO_2 adsorption.

More recently and taking advantage of photoelectron diffraction (PhD) [7] and NEXAFS [17] techniques, it was found that the formate species are adsorbed on the short-bridge sites of the Cu (100) and Cu (110) surfaces. The oxygen atoms are located at the same distance from the surface and with a Cu—O nearest-neighbour distance of 1.98 ± 0.04 Å.

For the Cu (111) surface, as far as we know, a similar PhD study does not exist. In a recent study [23] using IRAS for HCO_2/Cu (111), a bidentate structure was found with both oxygen atoms located at the same distance from the surface, thus possibly indicating adsorption of formate on the short-bridge site of the Cu (111) surface.

For low temperatures, it seems that this type of adsorption is preferred.

In the literature, only a few theoretical studies can be found on the adsorption of HCO_2 on copper surfaces [28–33]. These theoretical studies are 10 years old and use very poor methods (by today's standards) to evaluate chemisorption properties, with the exception of the recent studies of Casarin et al. [32] and Kakumoto et al. [33]. Casarin et al. [32] use a linear combination of atomic orbitals method within the local density approximation (LCAO–LDA) to study the chemisorption of formate on Cu (100). They studied the adsorption on the short-bridge and on the cross-bridge sites and concluded that the adsorption on the short-bridge site is the most favourable. Ab-initio MO calculations using the DFT method were presented by Kakumoto et al. [33] for the formate intermediate adsorbed on a $[Cu_2]^+$ bridge site. In this work, only the energy and geometry variation of the HCO_2 species with the Cu—Cu distance is calculated.

One of the goals of this paper is to compile theoretical results for the adsorption of the formate species on the Cu (100), (110) and (111) surfaces under the same conditions in terms of methodology and basis sets in order to compare the trends in the adsorption of this species.

This paper is organized as follows. In Section 2, the theoretical details are given for the computational method used and for the metal clusters used to describe the metal surface. In Section 3, the calculated results for HCO_2 adsorption on Cu (100), (110) and on Cu (111) surfaces are presented and in Section 4, a summary of the main conclusions obtained with this work is given.

2. Method

In the present work, the interaction of the formate species with copper (100), (110) and (111) surfaces is studied. For that purpose, the density functional theory (DFT) approach was used. The Cu (100) and the Cu (110) metal surfaces are modelled by a Cu_8 cluster and the Cu (111) surface by a Cu_7 cluster as shown in Fig. 1. These two-layer clusters are a small section of the ideal Cu (100), Cu (110) and Cu (111) surfaces with a Cu—Cu nearest-neighbour distance taken from

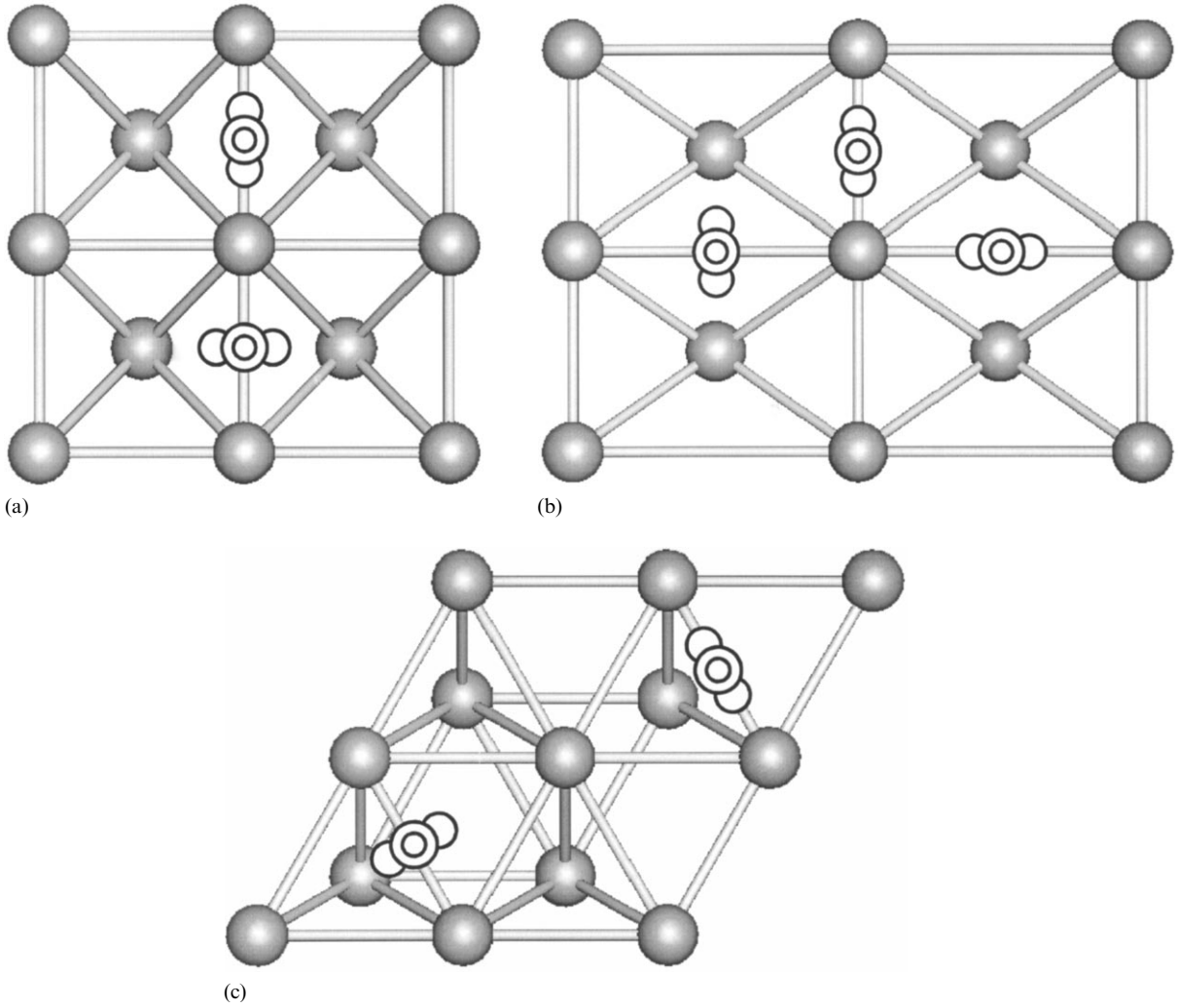

Fig. 1. Top views of the different sites studied on the (100), (110) and (111) copper surfaces. The (100) and (110) surfaces were modelled by a two-layer cluster with eight metal atoms. The (111) surface was modelled by a two-layer cluster with seven metal atoms. (a) (100) surface. (b) (110) surface. (c) (111) surface.

the bulk and equal to 2.551 Å. These clusters, albeit small, were found previously to give a reasonable description of the copper surface. In our experience, Cu_7 clusters for studying the methoxy [34,35] and dioxymethylene [36] adsorption on the copper (111) surface and Cu_n ($n=5$, 7, 12) clusters for studying halide ions [37,38] and water [39,40] adsorption on the copper (100) surface give very good results, which compare well with available experimental data. Also, in many catalytic real systems, it seems that copper exists as small islands above oxide media [24]. Larger clusters with a value of n up to 19 metal atoms were also used [34,38] in order to test these approximations.

The present calculations for the formate interaction with the copper surfaces were performed for short-bridge and cross-bridge orientations of the HCO_2 species, except for the Cu (110) surface where the long-bridge orientation was also studied. These orientations can be understood from Fig. 1. In the short-bridge site, the OCO group lies above a surface short bridge with its oxygen atoms point-

ing towards top sites, and in the cross-bridge site, the carbon atoms lies above the surface short bridge with the oxygen atoms pointing towards the hollow sites. In copper (100) and (110), these hollow sites are fourfold, whereas in the Cu (111) surface, they are threefold sites. For Cu (110), a HCO_2 long-bridge orientation was also studied where the OCO group is placed above a surface long-bridge site with the oxygen atoms pointing towards top sites.

The geometry of the adsorbed HCO_2 species was optimized in the calculations. Only one restriction was imposed during these optimizations, this being the conservation of the mirror plane that crosses the carbon, the oxygen and the copper atoms that define the long-, short- or cross-bridge sites. In all cases, the calculations were made with a starting geometry for the HCO_2 species with an equal surface–oxygen distance for both oxygen atoms. All calculations were made for the lowest spin multiplicity systems.

The DFT was used to obtain the geometry, energy and frequencies for the formate species adsorbed on the copper surfaces in the different orientations described above. The B3LYP hybrid method proposed by Becke [41] included in the Gaussian 94 [42] package was used. This method includes a mixture of Hartree–Fock (HF) and DFT exchange terms associated with the gradient corrected correlation functional of Lee et al. [43].

The metal atoms are described by the large LANL2DZ basis set, which treats the outer 19 electrons of copper atoms with a double zeta basis set and the inner 1s, 2s and 2p electrons with the effective core potential of Hay and Wadt [44]. The non-metallic atoms (O,C and H) are described by the 6-31G** basis set of double zeta quality with p polarization functions in hydrogen atoms and d polarization functions in carbon and oxygen atoms. Calculations were made only for the ground state configurations except for the free HCO_2 species where different electronic states were considered. The vibrational frequencies were obtained by calculation of the analytic second derivatives of the energy of the molecular systems, and an infinite mass was used for the copper atoms.

In order to test the validity of the systems studied, calculations for formate (HCO_2^-) adsorbed on the short-bridge site of a Cu_8 cluster and for HCO_2 adsorbed on the short-bridge site of a Cu_{18} cluster used to model the Cu (100) surface were also performed.

3. Results

3.1. Free HCO_2 and HCO_2^- species

Table 1 lists the computed geometry, energy and vibrational frequencies for the three different σ states of the HCOO radical, $^2B_2$, $^2A_1$ and $^2A'$ optimized at the DFT/6-31G** level. The calculations were made using as a starting point the geometry values obtained in previous work [45–47].

Depending on whether the oxygen atoms in HCO_2 are identical or not, there are two possible symmetric types for the HCO_2 species, C_{2v} and C_s. The $^2B_2$ and the $^2A_1$ states belong to the C_{2v} symmetric type, whereas the $^2A'$ state belongs to the C_s symmetric type.

The results show that the $^2B_2$ state has the lowest energy and the $^2A'$ state the second lowest (3.54 kJ mol^{-1} above $^2B_2$). The $^2A_1$ and the $^2A'$ states have a similar energy, with the $^2A_1$ state slightly more unstable. The computed OCO angle for the $^2B_2$ state is much smaller ($\sim 113^\circ$) than that found for the other two electronic states considered. For the $^2A_1$ and $^2A'$ states, the OCO angle is similar and approximately 143°. The π states are much more unstable. For example, the $^2B_1$ electronic state is 415 kJ mol^{-1} higher in energy than the $^2B_2$ electronic state. The $^2B_1$ electronic state is less stable, and this is in agreement with the values obtained by MCSCF [45], by HF and MP2 [46] and by CASSCF and CASPT2 [47]. The $^2B_2$ state was found to be the most stable electronic state by MP4, G2 and QCISD(T) [46] and by MRCI [47]. Using HF, MP2, CASSCF and CASPT2 [46,47], a minimum in energy was found also for the $^2A_1$ and $^2A'$ electronic states, and this is in agreement with the small difference in energy that we have observed for these three states.

Vibrational frequency calculations were also performed for these three electronic states, and the

Table 1
Geometry and energy (without ZPE corrections) of the optimized free HCO_2 and HCO_2^- species

Free species	HCO_2			HCO_2^-
	$^2B_2$	$^2A_1$	$^2A'$	$^1A_1$
Energy (a.u.)	−189.07695	−189.07559	−189.07560	−189.17445
Distance (CH) (Å)	1.1002	1.1554	1.1556	1.1536
Distance (CO_a) (Å)	1.2568	1.2311	1.2185	1.2542
Distance (CO_b) (Å)	1.2568	1.2311	1.2462	1.2542
Angle (O_aCO_b) (°)	113.05	143.78	143.37	131.10
Angle (O_aCH) (°)	123.48	108.08	113.02	114.45

results are shown in Table 2. They were found to be stationary points. However, the $^2A_1$ state is a transition structure with the imaginary frequency observed for the CH in-plane wagging. The same result was found by Feller et al. using the MCSCF procedure [45]. The small frequency value found for the C—H stretch for the $^2A_1$ and $^2A'$ states is due to the larger C—H bond length. The $^2A_1$ state is the saddle point that connects the $^2A'$ electronic state and the trans form of OCOH. This species is much more stable than any HCO_2 structure [45]. This reaction can also proceed by an intermediate step that is the formation of the dissociated H and CO_2 species and then the bonding of the hydrogen atom to one of the oxygen atom yielding OCOH.

The energy and geometry of the free anion were also obtained. The results for the most stable electronic state, $^1A_1$, of HCO_2^- are shown in Table 1. The values obtained for bond distances and angles lie between those obtained for the $^2B_2$ and $^2A_1$ states of the formyloxy species. The vibrational frequencies for the anion are shown in Table 2. The large C—H bond length is the cause of the small C—H stretch observed. The anion is $\approx$256 kJ mol^{-1} more stable than the radical.

Table 2
Vibrational frequencies (cm^{-1}) of HCO_2 and HCO_2^- species[a]

Free species	HCO_2			HCO_2^-
	$^2B_2$	$^2A_1$	$^2A'$	$^1A_1$
νf_1	647	680	699	764
νf_2	1033	858	861	1068
νf_3	1107	1652	1676	1777
νf_4	1301	265i	365	1415
νf_5	1509	1232	1210	1369
νf_6	3065	2407	2421	2468

[a] νf_1=OCO bending; νf_2=CH out-of-plane wagging; νf_3=CO asymmetric stretch; νf_4=CH in-plane wagging; νf_5=CO symmetric stretch; νf_6=CH stretch.

3.2. HCO_2/Cu (100)

Table 3 summarizes the computed geometry, adsorption energy and charge of the adsorbate for formate on the short-bridge and cross-bridge sites of the Cu (100) surface.

Formate bonds to the surface in two different forms. On the short-bridge site, formate binds to the surface in a bridge-bonded configuration, whereas on the cross-bridge site, it binds to the surface in a monodentate configuration. The HCO_2 species is stabilized more efficiently on the short-bridge site than on the cross-bridge site by approximately 56 kJ mol^{-1}. On the short-bridge site, both oxygen atoms interact directly with the surface, and they are located 2.014 Å from the metal surface. The C—O bonds are identical with the same bond length (1.266 Å). On the cross-bridge site, the two oxygen atoms are positioned at two different distances from the Cu (100) surface, i.e. 1.624 and 2.625 Å. The bond length between the formate carbon atom and the oxygen atom closer to the surface is larger (1.305 Å) than the bond length of the other C—O bond (1.230 Å). These bond lengths are consistent with a bond order of one and two, respectively [48]. For the adsorption on the short-bridge site, the calculated intermediate value indicates delocalization of charge density between the oxygen atoms.

Table 3
Adsorption energies (kJ mol^{-1}), optimized geometry and charges for HCO_2 adsorbed on the short-bridge and cross-bridge sites of the Cu (100) surface[a]

HCO_2/Cu (100)	Short-bridge	Cross-bridge
Adsorption energy (kJ mol^{-1})	−312.7	−256.5
Distance (CH) (Å)	1.103	1.108
Distance (CO_a) (Å)	1.266	1.305
Distance (CO_b) (Å)	1.266	1.230
Distance ($SurfO_a$) (Å)	2.014	1.624
Distance ($SurfO_b$) (Å)	2.014	2.625
Distance ($Cu_{sb}O_a$) (Å)	2.019	2.298
Distance (Cu_oO_a) (Å)	–	2.578
Distance ($Cu_{sb}O_b$) (Å)	2.019	3.087
Distance (Cu_oHO_b) (Å)	–	3.301
Angle (O_aCO_b) (°)	128.0	125.1
Angle (HCO_a) (°)	116.0	114.5
Angle (HCO_b) (°)	116.0	120.5
$q_{adsorbate}$ (Mulliken) (a.u.)	−0.34	−0.36
$q_{adsorbate}$ (NPA) (a.u.)	−0.73	−0.77
$q_{adsorbate}$ (MSK) (a.u.)	−0.33	−0.08
$q_{adsorbate}$ (CHG) (a.u.)	−0.51	−0.19

[a] The charge on the adsorbate was calculated using Mulliken, Natural Population Analysis (NPA), Merz–Singh–Kollman (MSK) and Breneman–Wiberg (CHG) atomic charges. The labels a and b are used to distinguish between the two oxygen atoms of HCO_2 adsorbed on the cross-bridge site. $Cu_{sb}O_a$ and $Cu_{sb}O_b$ denote the distance of the oxygen atoms to the short-bridge copper atoms. Cu_oO_a and Cu_oO_b denote the distance of the oxygen atoms to the other first-layer copper atoms used to define the hollow site. The experimental results for the CO and the CuO distances are 1.27 ± 0.04 Å [4] and 1.98 ± 0.04 Å [7], respectively. The experimental value for the OCO angle is $127\pm7°$ [4].

The calculated results for HCO_2 adsorption on the short-bridge site agree very well with the available experimental data [7], in which it was found that formate is adsorbed on the short-bridge site with a Cu—O distance of 1.98 ± 0.04 Å. The computed value lies in the experimental error bar, and the same happens with the C—O distance and the O—C—O angle, which were found experimentally [4] to be 1.27 ± 0.04 Å and $127\pm7°$ respectively. The geometry of the adsorbed formate is very similar to that obtained for the free HCO_2 species ($^2B_2$ state) except for the O—C—O angle, which is larger in the adsorbed species. This is probably due to the fact that with this geometry, the interaction with the metal atoms from the surface is larger, and also due to the donation of electron charge from the metal substrate to the adsorbate (see Table 3). The greater value observed in the O—C—O angle is due to the increase in the electron density near the oxygen atoms. In fact, this is consistent with the O—C—O angle calculated for the anion (see Table 1), where a charge of −1 is delocalized in the CO_2 group. Thus, the adsorbed HCO_2 species behaves like a mixture of the free HCO_2 and HCO_2^- species. The total charge in the adsorbate was calculated using four different types of atomic charges. When the Mulliken and Natural Population Analysis (NPA) methods were used, the total charge in the adsorbate was similar for the two sites studied and was different when the electrostatic potential derived charges [Merz–Singh–Kollman (MSK) and ChelpG (CHG) schemes] were used. The higher value is observed for the adsorption on the short-bridge site where the adsorption energy is higher. Since the O—C—O angle observed for the geometry of the adsorbed species is similar, the charge in the adsorbate for both sites should be similar. The MSK and CHG methods are not efficient to obtain total charges for small systems like those studied here.

The calculated vibrational frequencies are listed in Table 4. The agreement with the experimental results is good. The ν (CuO) stretching frequencies are higher for adsorption on the short-bridge site than on the cross-bridge site, indicating a stronger bond in the former case.

Table 4
Calculated vibrational frequencies for HCO_2 adsorption on the short-bridge and cross-bridge sites of the Cu (100) surface

HCO_2/Cu (100)	Short-bridge	Cross-bridge	Experimental
ν (CH)	3027	2968	2910[a], 2930[b]
ν_{assym} (OCO)	1604	1675	1640[a]
δ (OCH)	1394	1377	
ν_{sym} (OCO)	1372	1253	1330[a], 1325[b]
δ (OCH)	1048	1042	
ν (OCO)	765	753	760[a,b]
ν (OCu)	341	221	340[a], 320[b]
ν (OCu)	–	176	

[a] Ref. [1].
[b] Ref. [2].

3.3. HCO_2/Cu (110)

The results obtained for adsorption of the HCO_2 species on the Cu (110) surface are presented in Table 5. As was found for adsorption on the Cu (100) surface, the adsorption energy is higher if formate adsorbs on the short-bridge site. In this surface, the energy difference between adsorption on the short-bridge site and on the cross-bridge site is more important and is greater than 145 kJ mol^{-1}. The adsorption on the long-bridge site was also studied, and the adsorption energy is 280.9 kJ mol^{-1}.

The HCO_2 species binds to the short-bridge and long-bridge sites in a bridge-bonded conformation, whereas on the cross-bridge site, it binds in a monodentate way. The geometric parameters obtained for the two-bridge bonded conformations are very similar. The distances from the formate oxygen atoms to the nearest copper atoms are very similar, 2.030 Å for adsorption on the short-bridge site and 2.093 Å for adsorption on the long-bridge site, and this is not the reason for the observed large difference in the adsorption energy, approximately 66 kJ mol^{-1}.

This large difference must be due to the geometry of the oxygen atomic orbitals and the interacting atomic orbitals on the two neighbour copper atoms. The adsorption of the HCO_2 species on the copper surface involves mainly the oxygen 2p orbitals and the copper d orbitals (results not shown). The shorter distance for the two nearest-neighbour copper atoms on the short-bridge site of the Cu (110) surface is responsible for a higher interaction between the metallic orbitals, and this gives a stronger ligand effect.

The charge transferred from the metal surface is slightly higher than that observed for the same sites on the Cu (100) surface. Again, the Mulliken and NPA total charges are constant for the three sites considered for the (110) copper surface.

The calculated vibrational frequencies agree very well with the experimental frequencies (see Table 6). A better agreement is found for adsorption on the short-bridge site except the ν_{asym} (OCO) stretching mode for which the deviation is large

Table 5
Adsorption energies (kJ mol^{-1}), optimized geometry and charges for HCO_2 adsorbed on the short-bridge, long-bridge and cross-bridge sites of the Cu (110) surface[a]

HCO_2/Cu (110)	Short-bridge	Long-bridge	Cross-bridge
Adsorption energy (kJ mol^{-1})	−346.2	−280.9	−209.6
Distance (CH) (Å)	1.106	1.109	1.114
Distance (CO_a) (Å)	1.266	1.264	1.289
Distance (CO_b) (Å)	1.266	1.264	1.241
Distance ($SurfO_a$) (Å)	2.026	1.986	1.590
Distance ($SurfO_b$) (Å)	2.026	1.986	2.397
Distance ($Cu_{sb}O_a$) (Å)	2.030	2.093	2.626
Distance (Cu_oO_a) (Å)	–	–	2.832
Distance ($Cu_{sb}O_b$) (Å)	2.030	2.093	3.180
Distance (Cu_oO_b) (Å)	–	–	3.352
Angle (O_aCO_b) (°)	128.7	129.9	126.5
Angle (HCO_a) (°)	115.6	115.0	115.0
Angle (HCO_b) (°)	115.6	115.0	118.6
$q_{adsorbate}$ (Mulliken) (a.u.)	−0.40	−0.42	−0.42
$q_{adsorbate}$ (NPA) (a.u.)	−0.79	−0.80	−0.81
$q_{adsorbate}$ (MSK) (a.u.)	−0.43	−0.21	−0.24
$q_{adsorbate}$ (CHG) (a.u.)	−0.56	−0.32	−0.23

[a] The charge on the adsorbate was calculated using Mulliken, Natural Population Analysis (NPA), Merz–Singh–Kollman (MSK) and Breneman–Wiberg (CHG) atomic charges. The labels a and b are used to distinguish between the two oxygen atoms of HCO_2 adsorbed on the cross-bridge site. $Cu_{sb}O_a$ and $Cu_{sb}O_b$ denote the distance of the oxygen atoms to the short-bridge copper atoms. Cu_oO_a and Cu_oO_b denote the distance of the oxygen atoms to the other first-layer copper atoms used to define the hollow site. The experimental result for the the CuO distances is 1.98 ± 0.04 Å [7].

Table 6
Calculated vibrational frequencies for HCO_2 adsorption on the short-bridge, cross-bridge and cross-bridge sites of the Cu (110) surface

HCO_2/Cu (110)	Short-bridge	Long-bridge	Cross-bridge	Experimental[a]
ν (CH)	2990	2954	2892	2920, 2960
ν_{assym} (OCO)	1614	1603	1632	1560
δ (OCH)	1404	1414	1388	
ν_{sym} (OCO)	1373	1367	1298	1360
ρ (OCH)	1054	1049	1051	
δ (OCO)	762	728	737	780
ν (OCu)	332	261	171	390
ν (OCu)	–	259	133	

[a] Ref. [22].

($54\ cm^{-1}$). The large difference in Cu_{surf}—O stretching frequencies for adsorption on the cross-bridge site is consistent with a monodentate conformation for the adsorbed HCO_2 species.

3.4. HCO_2/Cu (111)

The calculated results for the HCO_2 adsorption on the Cu (111) surface are listed in Table 7. For the short-bridge site, a geometry of the formate species similar to those obtained for adsorption of HCO_2 on the same site on the Cu (100) and Cu (110) surfaces is observed. The Cu_{surf}—O distance is 2.015 Å, and this is very close to that calculated for adsorption on the Cu (100) surface (2.014 Å) and for adsorption on the Cu (110) surface (2.026 Å). The nearest-neighbour distance is 2.020 Å, which means that the oxygen atoms are atop two copper atoms of the short-bridge site. As far as we know, no experimental geometric results are available for adsorption of the HCO_2 species on the Cu (111) surface. Since the Cu—Cu distance for the Cu (111) short-bridge site is the same as those for the Cu (100) and Cu (110) surfaces, a comparison with the experimental results of Refs. [4,7] is made. The calculated O—Cu and C—O distances are 2.020 and 1.264 Å, respectively. These values are very similar to those obtained for the other two copper surfaces studied theoretically and experimentally [4,7]. The same is observed for the O—C—O angle, which is 127.8°.

The adsorption energy is $40\ kJ\ mol^{-1}$ higher for adsorption on the short-bridge site than on the cross-bridge site.

Table 7
Adsorption energies, optimized geometry and charges for HCO_2 adsorbed on the short-bridge and cross-bridge sites of the Cu (111) surface[a]

HCO_2/Cu (111)	Short-bridge	Cross-bridge
Adsorption energy ($kJ\ mol^{-1}$)	−329.2	−288.9
Distance (CH) (Å)	1.103	1.105
Distance (CO_a) (Å)	1.264	1.286
Distance (CO_b) (Å)	1.264	1.246
Distance ($SurfO_a$) (Å)	2.015	1.803
Distance ($SurfO_b$) (Å)	2.015	2.228
Distance ($Cu_{sb}O_a$) (Å)	2.020	2.472
Distance (Cu_oO_a) (Å)	–	2.111
Distance ($Cu_{sb}O_b$) (Å)	2.020	2.798
Distance (Cu_oO_b) (Å)	–	2.484
Angle (O_aCO_b) (°)	127.8	126.7
Angle (HCO_a) (°)	116.1	114.6
Angle (HCO_b) (°)	116.1	118.7
$q_{adsorbate}$ (Mulliken) (a.u.)	−0.33	−0.33
$q_{adsorbate}$ (NPA) (a.u.)	−0.70	−0.74
$q_{adsorbate}$ (MSK) (a.u.)	−0.09	−0.03
$q_{adsorbate}$ (CHG) (a.u.)	−0.38	−0.24

[a] The charge on the adsorbate was calculated using Mulliken, Natural Population Analysis (NPA), Merz–Singh–Kollman (MSK) and Breneman–Wiberg (CHG) atomic charges. The labels a and b are used to distinguish between the two oxygen atoms of HCO_2 adsorbed on the cross-bridge site. $Cu_{sb}O_a$ and $Cu_{sb}O_b$ denote the distance of the oxygen atoms to the short-bridge copper atoms. Cu_oO_a and Cu_oO_b denote the distance of the oxygen atoms to the other first-layer copper atoms used to define the hollow site.

The HCO_2 species adsorbs in a monodentate configuration with one oxygen atom of the

Table 8
Calculated vibrational frequencies for HCO_2 adsorption on the short-bridge and cross-bridge sites of the Cu (111) surface

HCO_2/Cu (111)	Short-bridge	Cross-bridge	Experimental[a]
ν (CH)	3032	3002	
ν_{assym} (OCO)	1603	1606	
δ (OCH)	1377	1375	
ν_{sym} (OCO)	1368	1331	1330
ρ (OCH)	1040	1036	
δ (OCO)	773	733	
ν (OCu)	323	254	
ν (OCu)	–	154	

[a] Ref. [23].

HCO_2 species located 1.863 Å from the surface and the other oxygen atom located 2.228 Å from the surface. The O—C—O angle is almost the same as that found for adsorption on the short-bridge site. The two C—O bonds have different bond lengths. As for adsorption on the Cu (110) surface, the difference in the two bond lengths is smaller than that observed for adsorption on the cross-bridge site of the Cu (100) surface.

The frequencies obtained for the adsorbed HCO_2 species on the Cu (111) surface are shown in Table 8. Again, similarity with the other two surfaces studied is observed. For adsorption on the cross-bridge site, the differences are higher. A red shift is observed in the O—C—O asymmetric stretch frequency when compared with the Cu (110) surface and especially with the Cu (100) surface. A reverse effect is observed for the O—C—O symmetric stretching frequency. This means that the difference in the two C—O bonds is higher for adsorption on the Cu (100) surface and that the difference in bond order effect is higher for the Cu (100) surface than for Cu (110) and Cu (111) surfaces.

The Cu—O stretch frequencies are higher for adsorption on the Cu (111) cross-bridge site when compared with the other two surfaces. This was to be expected since the adsorption energy difference between adsorption on the short-bridge and cross-bridge sites is smaller for the Cu (111) surface.

3.5. HCO_2 binding scheme to the copper surface

The adsorption of the HCO_2 species on the copper surfaces involves mainly the p orbitals of the adsorbate and the d orbitals of the metal surface. Upon adsorption, there is some charge transfer to the oxygen atoms and also to the carbon atom of the HCO_2 species. This is consistent with an ionic bond of HCO_2 to the copper surface. All calculations were performed for the adsorbed radical species since Olivera et al. [49] found that, after adsorption, the neutral and charged species would be the same entity. The infinite metal surface acts as an electron bath that accepts charge from the adsorbate or transfers charge to the adsorbate. In fact, this was observed in the system studied when small clusters were used. Table 9 shows the data obtained for the HCO_2^- adsorption on the short-bridge site of the Cu (100) surface. Small geometric differences were observed when the results were compared with the data obtained for the adsorbed radical species. The maximum deviation is reported for the O–surface distance ($\approx$0.06 Å). Due to the higher stability of the free anion when compared with the free radical, the adsorption energy is smaller for the anion adsorption. The total charge in the anion is similar to that obtained for the radical. The anion transfers electron charge to the metal surface, whereas the radical accepts electron charge from the metal surface. This is also confirmed by the linear behaviour of the dipole moment variation with the distance of the HCO_2 species to the metal surface (Fig. 2) for all the sites considered on the three copper surfaces studied. The component of the dipole moment normal to the surface is plotted against the distance of the substrate to the metal surface. This technique is based on the simple model of Bagus et al. [50–54]. For an ionic molecule represented by two point charges, $+q$ and $-q$, with the negative charge on the positive axis, the dipole moment is $\mu_z = -ql$, where l is the distance between the two point charges. Thus, the slope of the curve is $\delta\mu/\delta l = -q$. For a fully ionic molecule with $q=1$, $\delta\mu/\delta l = -1$, and the curve is a straight line. For ionic bonding, the slope is expected to be large, and the curvature is expected to be small. The slope of the curves is close to

Table 9
Adsorption energies (kJ mol^{-1}), optimized geometry and charges for HCO_2 adsorbed on the short-bridge of the Cu (100) surface[a]

Short-bridge	HCO_2/Cu_8	HCO_2/Cu_{18}	HCO_2^-/Cu_8
Adsorption energy (kJ mol^{-1})	−312.7	−318.4	−285.6
Distance (CH) (Å)	1.103	1.103	1.108
Distance (CO) (Å)	1.266	1.264	1.263
Distance (SurfO) (Å)	2.014	2.012	2.073
Distance ($Cu_{sb}O$) (Å)	2.019	2.017	2.077
Angle (OCO) (°)	128.0	128.2	128.6
Angle (HCO) (°)	116.0	115.9	115.7
$q_{adsorbate}$ (Mulliken) (a.u.)	−0.34	−0.31	−0.38
$q_{adsorbate}$ (NPA) (a.u.)	−0.73	−0.72	−0.76
$q_{adsorbate}$ (MSK) (a.u.)	−0.33	−0.68	−0.27
$q_{adsorbate}$ (CHG) (a.u.)	−0.51	−0.74	−0.62

[a] The charge on the adsorbate was calculated using Mulliken, Natural Population Analysis (NPA), Merz–Singh–Kollman (MSK) and Breneman–Wiberg (CHG) atomic charges. $Cu_{sb}O$ is the distance of the oxygen atoms to the short-bridge copper atoms. The experimental results for the CO and the CuO distances are 1.27 ± 0.04 Å [4] and 1.98 ± 0.04 Å [7], respectively. The experimental value for the OCO angle is $127 \pm 7°$ [4].

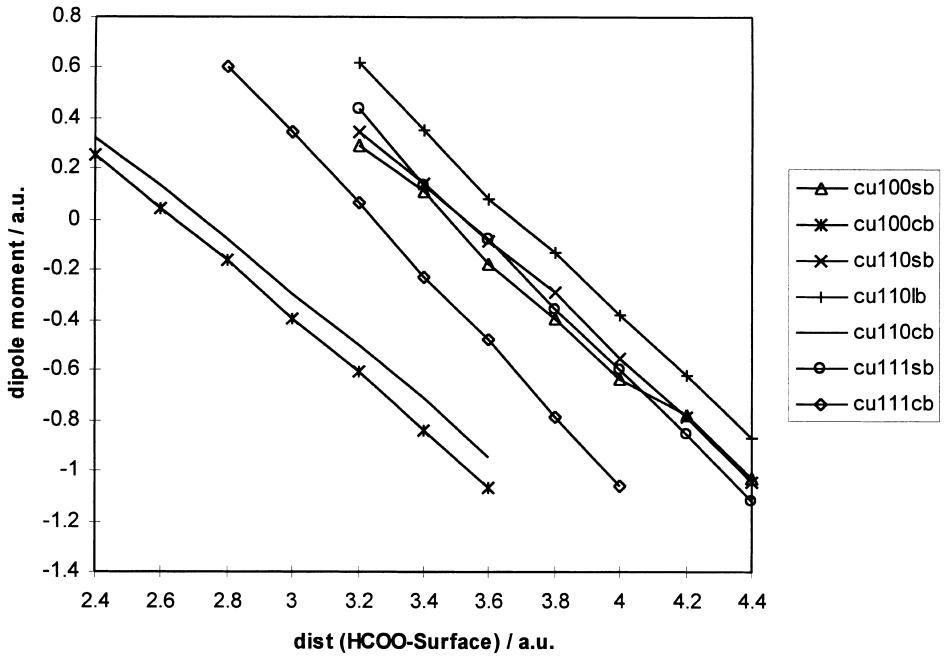

Fig. 2. Dipole moment variation with the distance from the copper (100), (110) and (111) surfaces to the HCO_2 species adsorbed on the short-bridge, long-bridge and cross-bridge sites. The curves were obtained for $z \pm 0.6$ a. u. adsorbate–surface distances with z equal to the equilibrium distance.

−1.1. This value is larger than the charges obtained with the different schemes employed to obtain the total charge in the adsorbate. This was expected since the influence of the adsorbate approaching the surface is not considered (cluster polarization). From the curves plotted in Fig. 2, it is concluded that the binding of the formate species to the copper surface is independent of the site

and of the surface. This is in disagreement with the total charges obtained with the electrostatic potential derived charges for the Cu_7 and Cu_8 clusters. Mulliken charges are known to give an underestimation of total charges. For a negative charge placed above a hollow or a top site of the Pt (111) surface, Garcìa-Hernández et al. [55] observed that the model of Bagus et al. [50–54] gives charges in the adsorbate greater than the real charges by 35-40%. This finding is in agreement with the NPA total charge obtained with all the metal clusters and with the CHG and MSK total charges obtained with the Cu_{18} cluster (see Table 9).

4. Conclusions

The ab-initio cluster model approach has been applied to study the adsorption of the HCO_2 species on the copper (100), (110) and (111) surfaces. Small metal clusters of seven and eight metal atoms have been chosen to model the short-bridge, long-bridge and cross-bridge sites in the three metallic surfaces as these have been shown to be trustworthy for studies of this type. In order to justify the use of these small clusters in this work, we have also studied HCO_2 adsorption on the short-bridge site of a Cu_{18} (12,6) cluster where the short-bridge site is surrounded by one neighbour atom in all directions on and below the surface. This cluster was used to model the Cu (100) surface. The results obtained are shown in Table 9 and compared with the results obtained with the Cu_8 (6,2) cluster. The differences are very small; for the bond lengths, the maximum difference is 0.002 Å, and for the internal angles, it is 0.2°; for the adsorption energy, the difference is ≈ 6 kJ mol^{-1}. Surprisingly, the MSK and CHG charges are similar to those obtained with the NPA method. Thus, for our small systems, the number of point charges used to fit the electrostatic potential by the MSK and the CHG methods is small. The results obtained agree well with the experimental data available for the Cu (100) and Cu (110) surfaces. It is observed that the adsorption geometry, adsorption energy and vibrational frequencies obtained for the Cu (111) surface are similar to those obtained for the Cu (100) and Cu (110) surfaces. The formate species is preferentially adsorbed on the short-bridge site of these surfaces. The adsorption energies range from 310 to 350 kJ mol^{-1} for the radical adsorption and are smaller for the anion adsorption. Due to the great stability of the formate species on the copper surfaces considered, the formic acid adsorption yields O—H bond scission, which is preferred to C—O bond breaking. This preference leads to the dehydrogenation reaction instead of the dehydration reaction with production of adsorbed HCO and OH. To obtain the adsorption energy of the adsorbed species, the energy values of the isolated HCO_2 and HCO_2^- species were needed. Three σ electronic states of this species were studied: the $^2B_2$, $^2A_1$ and $^2A'$ electronic states. The π states were not extensively studied because these states are much higher in energy. It was found that the $^2B_2$ state is the ground state of the HCO_2 species. This is in agreement with other theoretical results [45–47]. The calculated vibrational frequencies show that the $^2A_1$ electronic state is a transition state. Its geometry is very similar to that obtained for the $^2A'$ electronic state. The $^2A_1$ state is a transition structure that connects the $^2A'$ state and the OCOH form, which was found previously [45] to be more stable than any HCO_2 structure. Only the $^1A_1$ state of the HCO_2^- species was studied. This species is much more stable than the HCO_2 radical.

The adsorbed HCO_2 has a higher O—C—O angle when compared with the gas form. This is due to the donation of charge from the metal surface, and at the same time, this makes the interaction with the copper surface more efficient.

Acknowledgements

Financial support from the Fundação para a Ciência e Tecnologia (Lisbon) and project PRAXIS/PCEX/C/QUI/61/96 is acknowledged. J.R.B.G. thanks PRAXIS for a doctoral scholarship (BD/5522/95). We thank Professor Francesc Illas for helpful discussions.

References

[1] B.A. Sexton, Surf. Sci. 88 (1979) 319.
[2] L.H. Dubois, T.H. Ellis, B.R. Zegarski, S.D. Kevan, Surf. Sci. 172 (1986) 385.
[3] J. Stohr, D. Outka, R.J. Madix, U. Dobler, Phys. Rev. Lett. 54 (1985) 1256.
[4] D. Outka, R.J. Madix, J. Stohr, Surf. Sci. 164 (1985) 235.
[5] M.D. Crapper, C.E. Riley, D.P. Woodruff, Phys. Rev. Lett. 57 (1986) 2598.
[6] M.D. Crapper, C.E. Riley, D.P. Woodruff, Surf. Sci. 184 (1987) 121.
[7] D.P. Woodruff, C.F. McConville, A.L.D. Kilcoyne, Th. Lindner, J. Somers, M. Surman, G. Paolucci, A.M. Bradshaw, Surf. Sci. 201 (1988) 228–244.
[8] D.H.S. Ying, R.J. Madix, J. Catal. 61 (1980) 48.
[9] M. Bowker, R.J. Madix, Surf. Sci. 102 (1981) 542.
[10] B.E. Hayden, K. Prince, D.P. Woodruff, A.M. Bradshaw, Surf. Sci. 133 (1983) 589.
[11] B.E. Hayden, K. Prince, D.P. Woodruff, A.M. Bradshaw, Phys. Rev. Lett. 51 (1983) 475.
[12] M. Bowker, E. Rowbotham, F.M. Leibsle, S. Haq, Surf. Sci. 349 (1996) 97.
[13] S. Poulstoon, A. Jones, R.A. Bennett, M. Bowker, Surf. Sci. 377–379 (1997) 66.
[14] A.H. Jones, S. Poulston, R.A. Bennett, M. Bowker, Surf. Sci. 380 (1997) 31.
[15] A. Puschmann, J. Haase, M.D. Crapper, C.E. Riley, D.P. Woodruff, Phys. Rev. Lett. 54 (1985) 2250.
[16] M.D. Crapper, C.E. Riley, D.P. Woodruff, A. Puschmann, J. Haase, Surf. Sci. 171 (1986) 1.
[17] J. Somers, A.W. Robinson, Th. Lindner, D. Ricken, A.M. Bradshaw, Phys. Rev. B 40 (1989) 2053.
[18] F.C. Henn, J.A. Rodriguez, C.T. Campbell, Surf. Sci. 236 (1990) 282.
[19] P. Hofmann, D. Menzel, Surf. Sci. 191 (1987) 353.
[20] S. Haq, F.M. Leibsle, Surf. Sci. 375 (1997) 81.
[21] A.F. Carley, P.R. Davies, G.G. Mariotti, Surf. Sci. 401 (1998) 400.
[22] B.A. Sexton, A.E. Hughes, N.R. Avery, Surf. Sci. 155 (1985) 366.
[23] I. Nakamura, H. Nakano, T. Fujitami, T. Uchijima, J. Nakamura, Surf. Sci. 402–404 (1998) 92.
[24] G.J. Millar, C.H. Rochester, K.C. Waugh, J. Chem. Soc. Faraday Trans. 87 (1991) 1491.
[25] J. Yoshihara, C.T. Campbell, Surf. Sci. 407 (1998) 256.
[26] G. Thornton, S. Crook, Z. Chang, Surf. Sci. 415 (1998) 122.
[27] J.F. Edwards, G.L. Schrader, J. Phys. Chem. 89 (1985) 782.
[28] D.W. Bullet, W.G. Dawson, Prog. Surf. Sci. 25 (1987) 275.
[29] J.A. Rodriguez, C.T. Campbell, Surf. Sci. 183 (1987) 449.
[30] A. Wander, B.W. Holland, Surf. Sci. 199 (1988) L403.
[31] S.P. Mehandru, A.B. Andreson, Surf. Sci. 219 (1989) 68.
[32] M. Casarin, G. Granozzi, M. Sambi, E. Tondello, A. Vittadini, Surf. Sci. 307–309 (1994) 95.
[33] T. Kakumoto, T. Watanabe, Catal. Today 36 (1997) 39.
[34] J.R.B. Gomes, J.A.N.F. Gomes, J. Mol. Struct. Theochem. 463 (1999) 163.
[35] J.R.B. Gomes, J.A.N.F. Gomes, Electrochim. Acta, in press.
[36] J.R.B. Gomes, J.A.N.F. Gomes, submitted.
[37] A. Ignaczak, J.A.N.F. Gomes, Chem. Phys. Lett. 257 (1996) 609.
[38] A. Ignaczak, J.A.N.F. Gomes, J. Electroanal. Chem. 420 (1997) 71.
[39] A. Ignaczak, J.A.N.F. Gomes, J. Electroanal. Chem. 420 (1997) 209.
[40] A. Ignaczak, J.A.N.F. Gomes, in: P. Braunstein, L.A. Oro, P.R. Raithby (Eds.), Metal Clusters in Chemistry, Wiley-VCH, pp. 1549, to be published.
[41] A.D. Becke, J. Chem. Phys. 98 (1993) 5648.
[42] M.J. Frisch, G.W. Trucks, H.B. Schlegel, P.M.W. Gill, B.G. Johnson, M.A. Robb, J.R. Cheeseman, T. Keith, G.A. Petersson, J.A. Montgomery, K. Raghavachari, M.A. Al-Laham, V.G. Zakrzewski, J.V. Ortiz, J.B. Foresman, J. Cioslowski, B.B. Stefanov, A. Nanayakkara, M. Challacombe, C.Y. Peng, P.Y. Ayala, W. Chen, M.W. Wong, J.L. Andres, E.S. Replogle, R. Gomperts, R.L. Martin, D.J. Fox, J.S. Binkley, D.J. Defrees, J. Baker, J.P. Stewart, M. Head-Gordon, C. Gonzalez, J.A Pople, Gaussian 94, Gaussian, Pittsburgh, PA, 1995. Revision D.4.
[43] C. Lee, W. Yang, R.G. Parr, Phys. Rev. B 37 (1980) 785.
[44] P.J. Hay, W.R. Wadt, J. Chem. Phys. 82 (1985) 270.
[45] D. Feller, E.S. Huyser, W.T. Borden, E.R. Davidson, J. Am. Chem. Soc. 105 (1983) 1459.
[46] A. Rauk, D. Yu, D.A. Armstrong, J. Am. Chem. Soc. 116 (1994) 8222.
[47] A. Rauk, D. Yu, P. Borowski, B. Roos, Chem. Phys. 197 (1995) 73.
[48] Interatomic Distances Supplement, The Chemical Society, London, 1965.
[49] P.P. Olivera, E.M. Patrito, H. Sellers, E. Schustorovic, J. Mol. Catal. A: Chem. 119 (1997) 275.
[50] C.J. Nelin, P.S. Bagus, M.R. Philpott, J. Chem. Phys. 87 (1987) 2170.
[51] P.S. Bagus, G. Pacchioni, M.R. Philpott, J. Chem. Phys. 90 (1989) 4287.
[52] G. Pacchioni, P.S. Bagus, M.R. Philpott, Z. Phys. D 12 (1989) 543.
[53] G. Pacchioni, P.S. Bagus, M.R. Philpott, C.J. Nelin, Int. J. Quantum Chem. 38 (1990) 675.
[54] P.S. Bagus, F. Illas, Phys. Rev. B 42 (1990) 10852.
[55] M. Garcia-Hernández, P.S. Bagus, F. Illas, Surf. Sci. 409 (1998) 69.